DI22A-08

# Dynamics of ULVZ-mantle interaction using fast multipole boundary element method

NSF EAR 0911094 and EAR 1215800

Tyler Drombosky - drombosk@math.umd.edu

University of Maryland College Park

Applied Mathematics and Scientific Computation

Saswata Hier-Majumder - saswata@umd.edu

University of Maryland College Park

Department of Geology

Center for Computational Sciences and Mathematical Modeling

# The UltraLow Velocity Zones

- 3:1 s-wave to p-wave loss in velocity
- 50-100 km wide
- 10-40 km thick
- 1-2 orders of magnitude less viscous
- 10% more dense
- Dynamically coupled to surrounding mantle

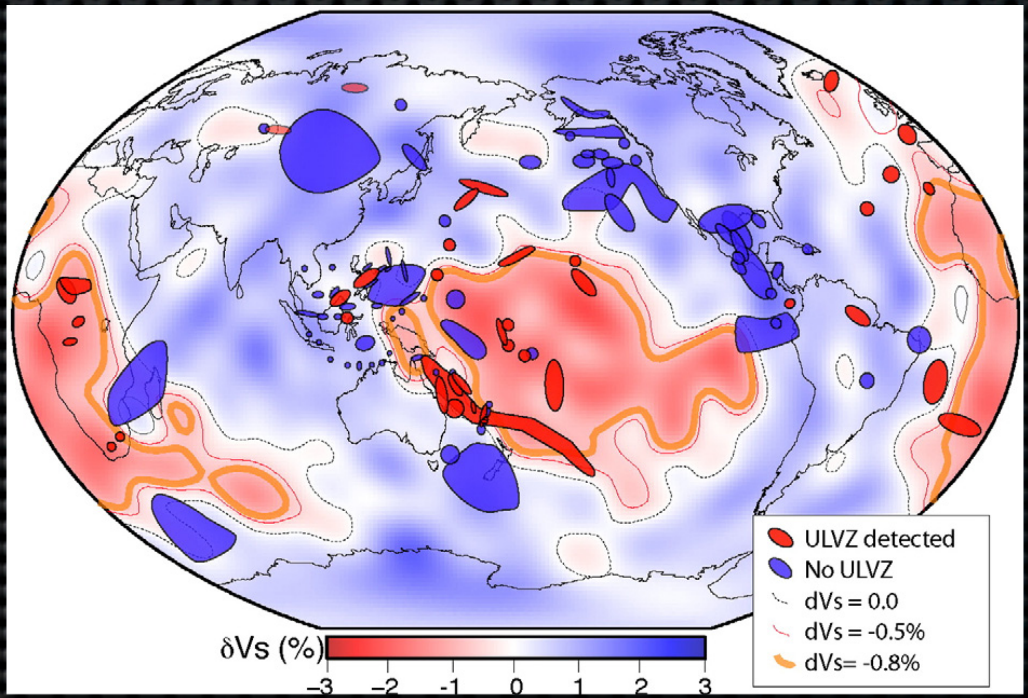


[McNarama et al. 2010]

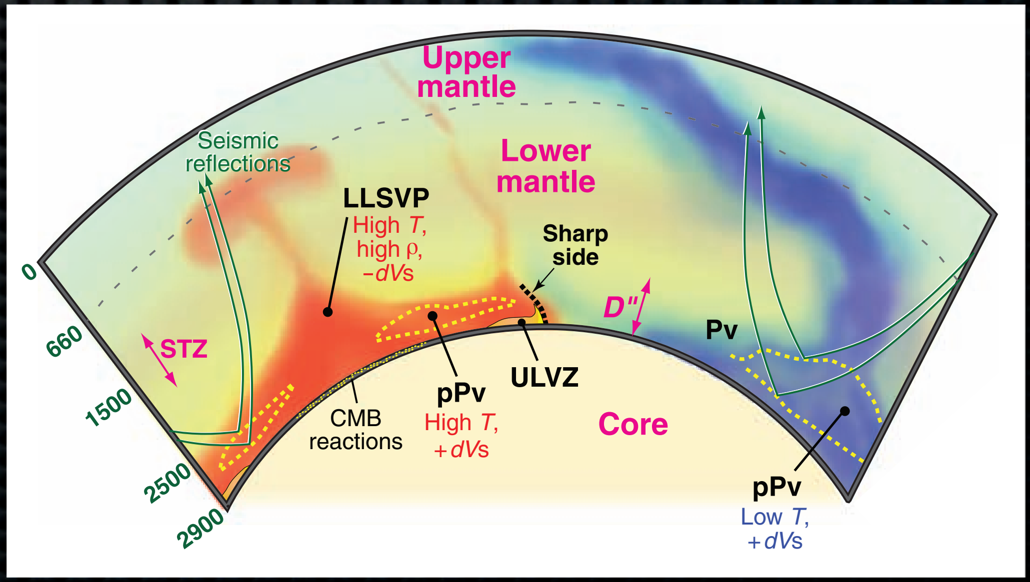


[Garnero and McNarama 2008]

# Experimental Model

- Forcing terms
  - Buoyancy
  - Imposed velocity field (flow within LLSVP)
- Modulating terms
  - Viscosity ratio varies patches desire to deform
- Patch interaction

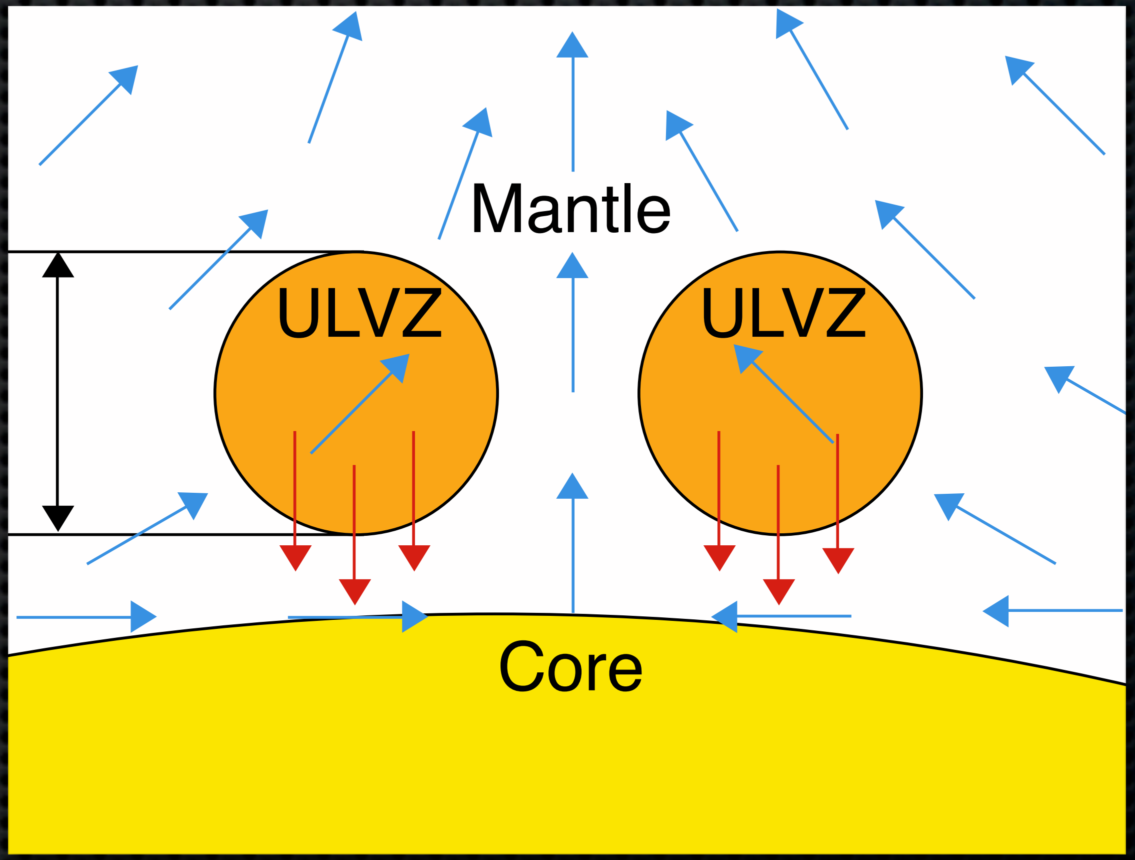

# Experimental Model

- Forcing terms
  - Buoyancy
  - Imposed velocity field (flow within LLSVP)
- Modulating terms
  - Viscosity ratio varies patches desire to deform
- Patch interaction

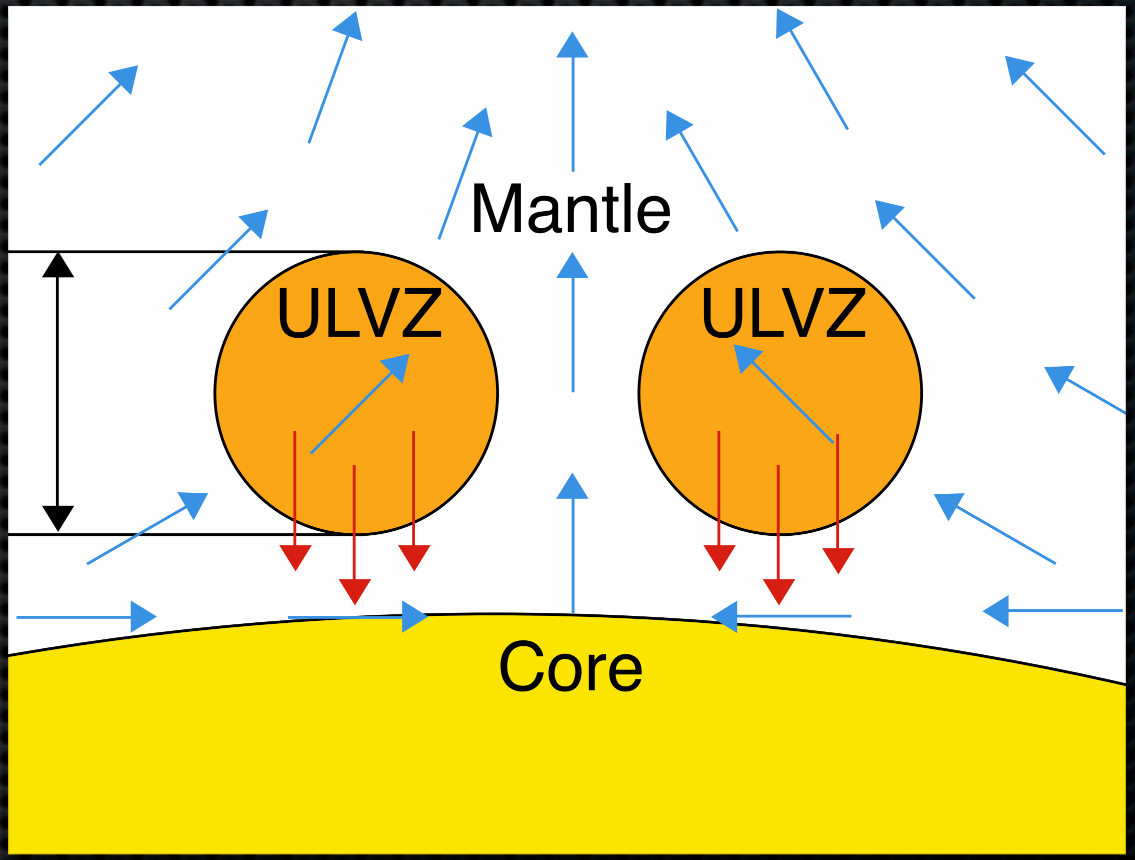


What is the drainage rate of the ULVZ?

# Governing Equation

- The Stokes Boundary Integral Equation (BIE) for multiple domains [Pozrikidis 2001]

$$\frac{1+\lambda_q}{2} u_j(\boldsymbol{x}) = u_j^\infty(\boldsymbol{x}_0) - \sum_{p=1}^{P} \frac{\mathcal{R}_p}{4\pi} \int_{\Gamma_p} \Delta f_i^{(p)}(\boldsymbol{x}) U_{ij}(\boldsymbol{x}, \boldsymbol{x}_0) \, \mathrm{d}\Gamma_m(\boldsymbol{x})$$

$$+ \sum_{p=1}^{P} \frac{1-\lambda_p}{4\pi} \int_{\Gamma_p}^{\mathcal{PV}} u_i(\boldsymbol{x}) T_{ijk}(\boldsymbol{x}, \boldsymbol{x}_0) \hat{n}_k(\boldsymbol{x}) \, \mathrm{d}\Gamma_p(\boldsymbol{x})$$

- The interfacial surface term is buoyancy driven

$$\mathcal{R}^{(p)} = \frac{(\rho_m - \rho_p) g x_c^2}{u_c \mu_m} \qquad \lambda_p = \frac{\mu_p}{\mu_m}$$

- Non-dimensionalizion yields the viscosity ratio and compositional Rayleigh number [Leal 2007]

# Governing Equation

- The Stokes Boundary Integral Equation (BIE) for multiple domains [Pozrikidis 2001]

$$\frac{1+\lambda_q}{2} u_j(\boldsymbol{x}) = \boxed{u_j^\infty(\boldsymbol{x}_0)} - \sum_{p=1}^{P} \frac{\mathcal{R}_p}{4\pi} \int_{\Gamma_p} \Delta f_i^{(p)}(\boldsymbol{x}) U_{ij}(\boldsymbol{x}, \boldsymbol{x}_0)\, \mathrm{d}\Gamma_m(\boldsymbol{x})$$

$$+ \sum_{p=1}^{P} \frac{1-\lambda_p}{4\pi} \int_{\Gamma_p}^{\mathcal{PV}} u_i(\boldsymbol{x}) T_{ijk}(\boldsymbol{x}, \boldsymbol{x}_0) \hat{n}_k(\boldsymbol{x})\, \mathrm{d}\Gamma_p(\boldsymbol{x})$$

- The interfacial surface term is buoyancy driven

$$\mathcal{R}^{(p)} = \frac{(\rho_m - \rho_p) g x_c^2}{u_c \mu_m} \qquad \lambda_p = \frac{\mu_p}{\mu_m}$$

- Non-dimensionalizion yields the viscosity ratio and compositional Rayleigh number [Leal 2007]

# Governing Equation

- The Stokes Boundary Integral Equation (BIE) for multiple domains [Pozrikidis 2001]

$$\frac{1+\lambda_q}{2} u_j(\boldsymbol{x}) = u_j^{\infty}(\boldsymbol{x}_0) - \sum_{p=1}^{P} \frac{\mathcal{R}_p}{4\pi} \int_{\Gamma_p} \Delta f_i^{(p)}(\boldsymbol{x}) U_{ij}(\boldsymbol{x}, \boldsymbol{x}_0)\, \mathrm{d}\Gamma_m(\boldsymbol{x})$$

$$+ \sum_{p=1}^{P} \frac{1-\lambda_p}{4\pi} \int_{\Gamma_p}^{\mathcal{PV}} u_i(\boldsymbol{x}) T_{ijk}(\boldsymbol{x}, \boldsymbol{x}_0) \hat{n}_k(\boldsymbol{x})\, \mathrm{d}\Gamma_p(\boldsymbol{x})$$

- The interfacial surface term is buoyancy driven

$$\mathcal{R}^{(p)} = \frac{(\rho_m - \rho_p) g x_c^2}{u_c \mu_m} \qquad \lambda_p = \frac{\mu_p}{\mu_m}$$

- Non-dimensionalizion yields the viscosity ratio and compositional Rayleigh number [Leal 2007]

# Governing Equation

- The Stokes Boundary Integral Equation (BIE) for multiple domains [Pozrikidis 2001]

$$\frac{1+\lambda_q}{2} u_j(\boldsymbol{x}) = u_j^{\infty}(\boldsymbol{x}_0) - \sum_{p=1}^{P} \frac{\mathcal{R}_p}{4\pi} \int_{\Gamma_p} \Delta f_i^{(p)}(\boldsymbol{x}) U_{ij}(\boldsymbol{x}, \boldsymbol{x}_0)\, \mathrm{d}\Gamma_m(\boldsymbol{x})$$

$$+ \sum_{p=1}^{P} \frac{1-\lambda_p}{4\pi} \int_{\Gamma_p}^{\mathcal{PV}} u_i(\boldsymbol{x}) T_{ijk}(\boldsymbol{x}, \boldsymbol{x}_0) \hat{n}_k(\boldsymbol{x})\, \mathrm{d}\Gamma_p(\boldsymbol{x})$$

- The interfacial surface term is buoyancy driven

$$\mathcal{R}^{(p)} = \frac{(\rho_m - \rho_p) g x_c^2}{u_c \mu_m} \qquad \lambda_p = \frac{\mu_p}{\mu_m}$$

- Non-dimensionalizion yields the viscosity ratio and compositional Rayleigh number [Leal 2007]

# Governing Equation

- The Stokes Boundary Integral Equation (BIE) for multiple domains [Pozrikidis 2001]

$$\frac{1+\lambda_q}{2} u_j(\boldsymbol{x}) = \boxed{u_j^\infty(\boldsymbol{x}_0)} - \boxed{\sum_{p=1}^{P} \frac{\mathcal{R}_p}{4\pi} \int_{\Gamma_p} \Delta f_i^{(p)}(\boldsymbol{x}) U_{ij}(\boldsymbol{x}, \boldsymbol{x}_0) \, \mathrm{d}\Gamma_m(\boldsymbol{x})}$$

$$+ \boxed{\sum_{p=1}^{P} \frac{1-\lambda_p}{4\pi} \int_{\Gamma_p}^{\mathcal{PV}} u_i(\boldsymbol{x}) T_{ijk}(\boldsymbol{x}, \boldsymbol{x}_0) \hat{n}_k(\boldsymbol{x}) \, \mathrm{d}\Gamma_p(\boldsymbol{x})}$$

- The interfacial surface term is buoyancy driven

$$\boxed{\mathcal{R}^{(p)} = \frac{(\rho_m - \rho_p) g x_c^2}{u_c \mu_m}} \qquad \lambda_p = \frac{\mu_p}{\mu_m}$$

- Non-dimensionalizion yields the viscosity ratio and compositional Rayleigh number [Leal 2007]

# Governing Equation

- The Stokes Boundary Integral Equation (BIE) for multiple domains [Pozrikidis 2001]

$$\frac{1+\lambda_q}{2} u_j(\boldsymbol{x}) = u_j^{\infty}(\boldsymbol{x}_0) - \sum_{p=1}^{P} \frac{\mathcal{R}_p}{4\pi} \int_{\Gamma_p} \Delta f_i^{(p)}(\boldsymbol{x}) U_{ij}(\boldsymbol{x}, \boldsymbol{x}_0)\, \mathrm{d}\Gamma_m(\boldsymbol{x})$$

$$+ \sum_{p=1}^{P} \frac{1-\lambda_p}{4\pi} \int_{\Gamma_p}^{\mathcal{PV}} u_i(\boldsymbol{x}) T_{ijk}(\boldsymbol{x}, \boldsymbol{x}_0) \hat{n}_k(\boldsymbol{x})\, \mathrm{d}\Gamma_p(\boldsymbol{x})$$

- The interfacial surface term is buoyancy driven

$$\mathcal{R}^{(p)} = \frac{(\rho_m - \rho_p) g x_c^2}{u_c \mu_m} \qquad \lambda_p = \frac{\mu_p}{\mu_m}$$

- Non-dimensionalizion yields the viscosity ratio and compositional Rayleigh number [Leal 2007]

# Numerical Method

- Collocation
- Cubic spline interpolation for geometry
- Gaussian quadrature or RIM2D (singular) integration
- Generally dense and asymmetric

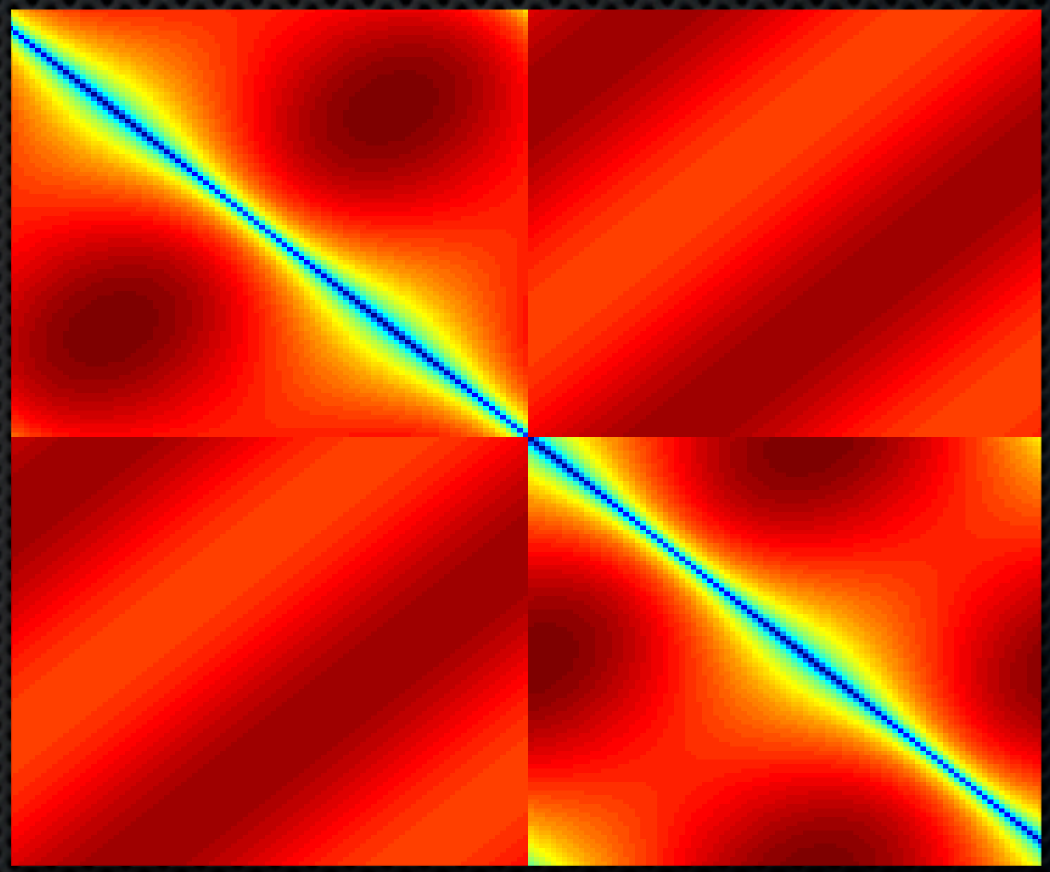

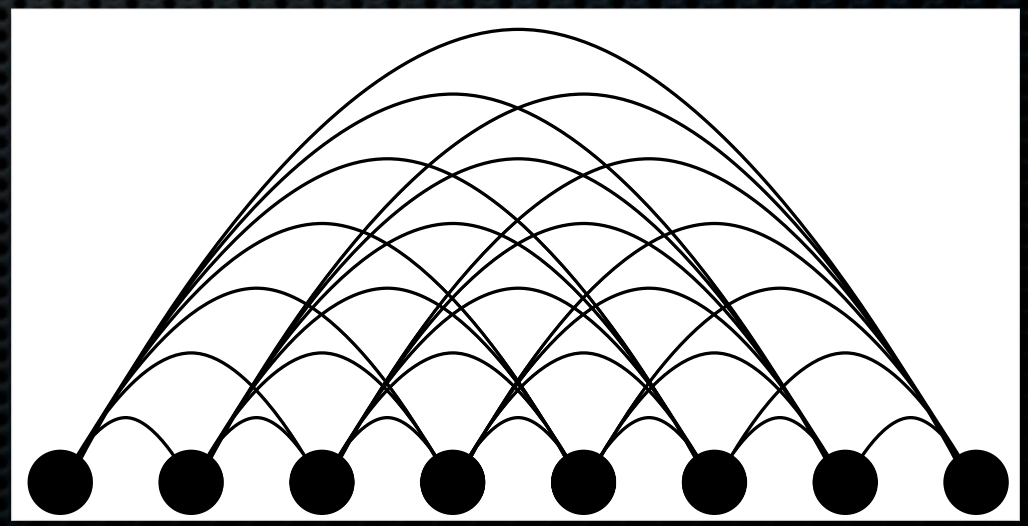

# Fast Multipole Method

- Approximate the integral over a boundary element
- Move series expansions up and down a tree
  - Translate
  - Combine
- Distant interactions represented by a series
- Nearby interactions are computed directly

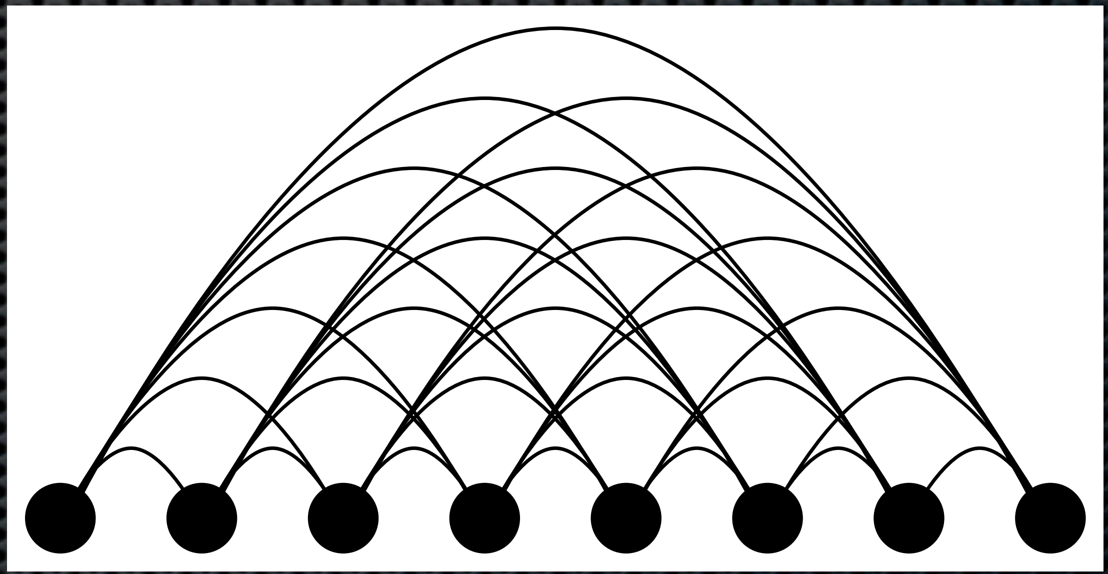

Direct Method

- Tree structure results in $\mathcal{O}(N \log N)$ iterative method

# Fast Multipole Method

- Approximate the integral over a boundary element
- Move series expansions up and down a tree
  - Translate
  - Combine
- Distant interactions represented by a series
- Nearby interactions are computed directly

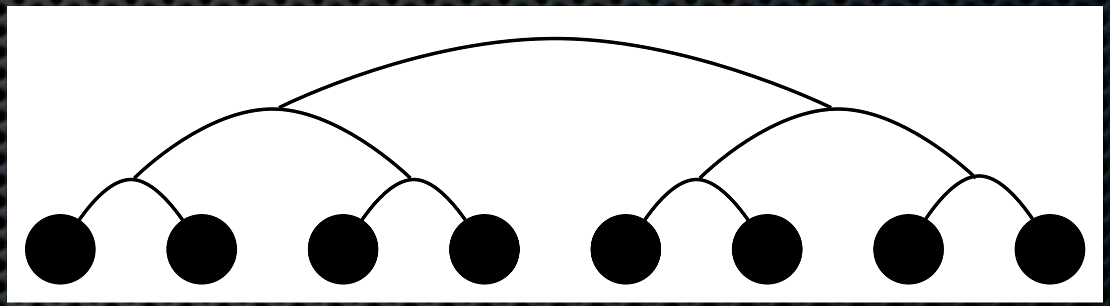

Fast Method

- Tree structure results in $O(N \log N)$ iterative method

# ULVZ Simulation #1

- Buoyancy Driven System
- No Imposed Velocity

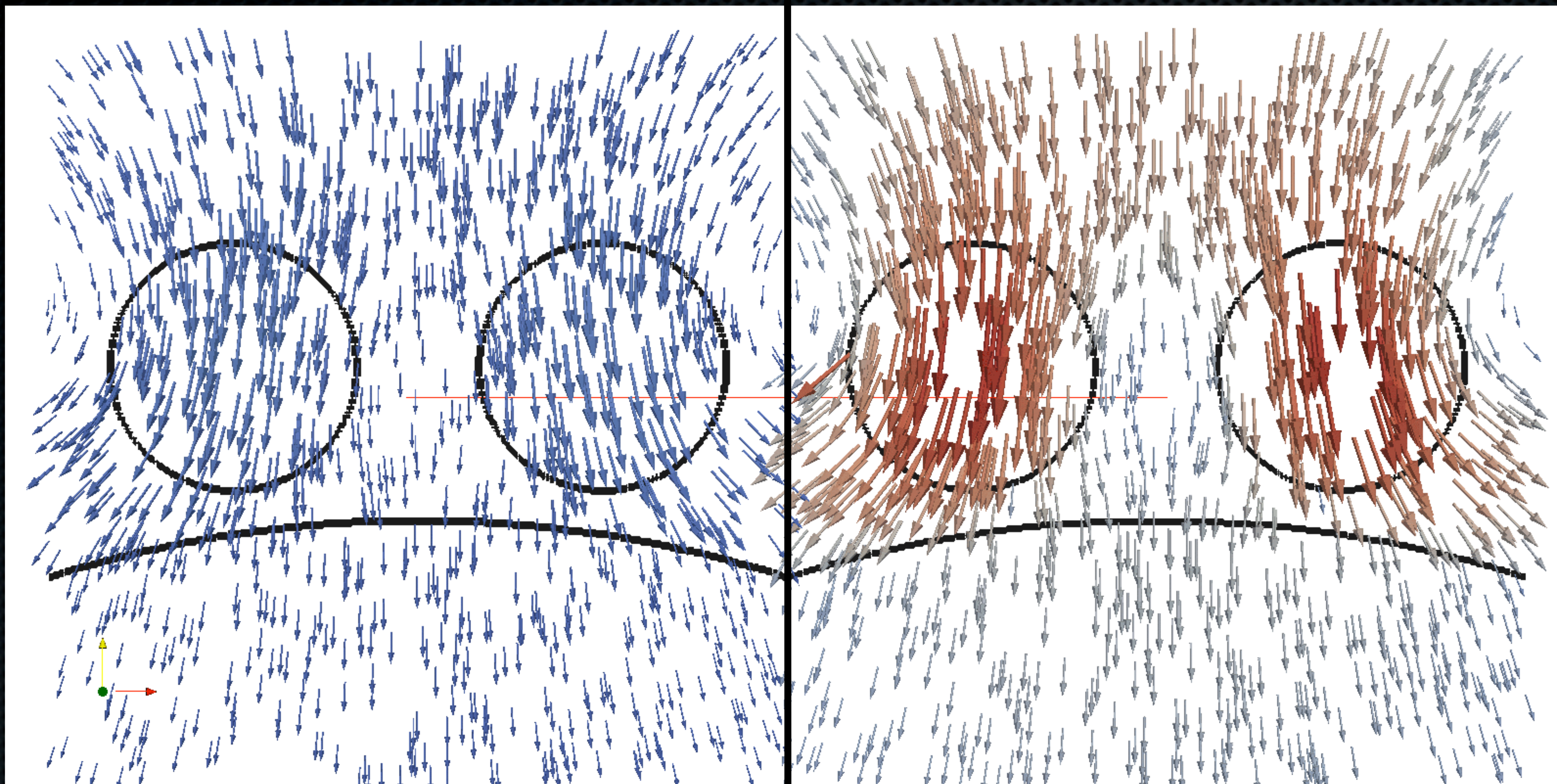

# ULVZ Dynamics (5 Myrs)

Left: High patch viscosity, low buoyancy force

Right: Low patch viscosity, high buoyancy force

# Patch Settling

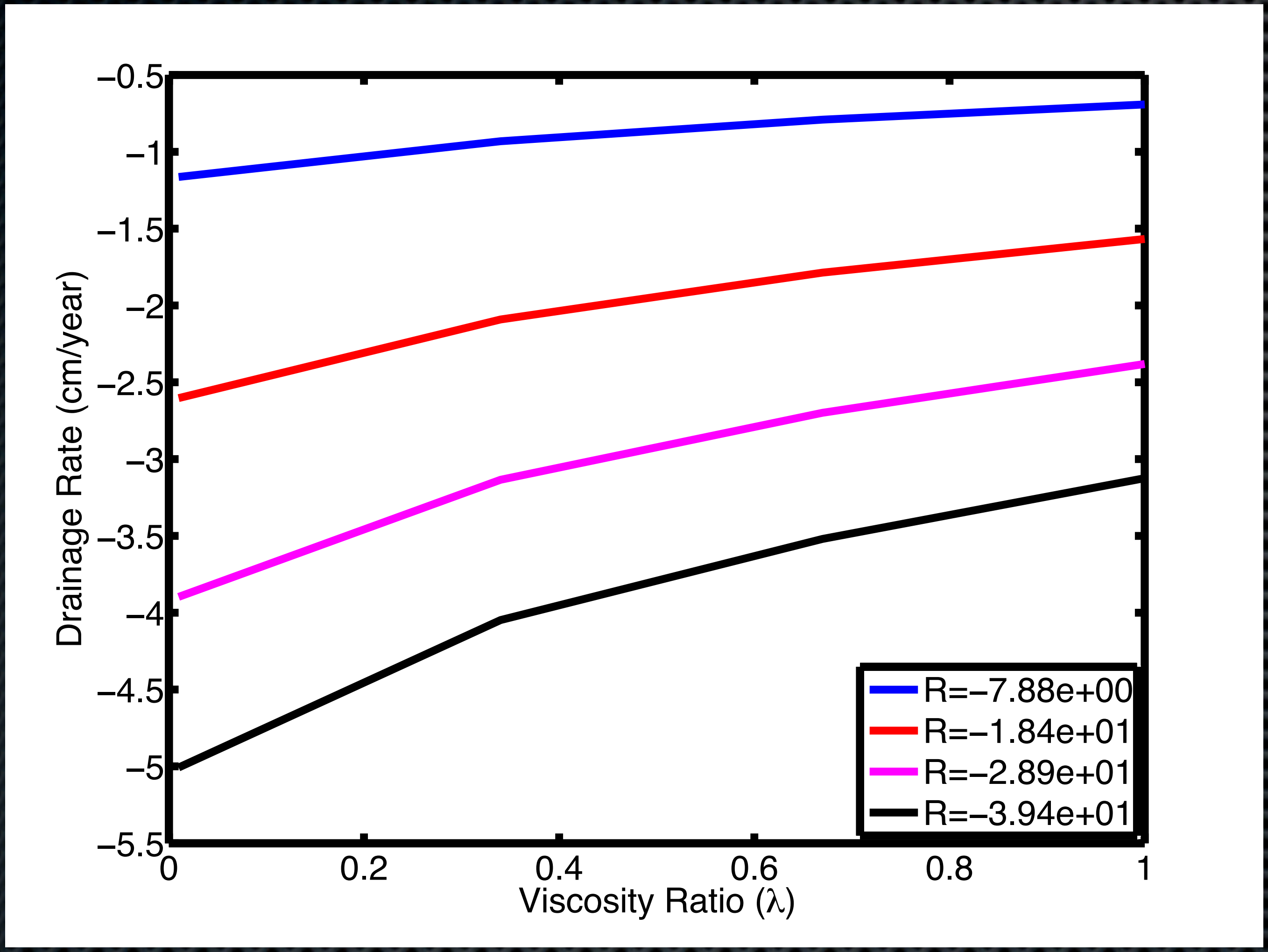


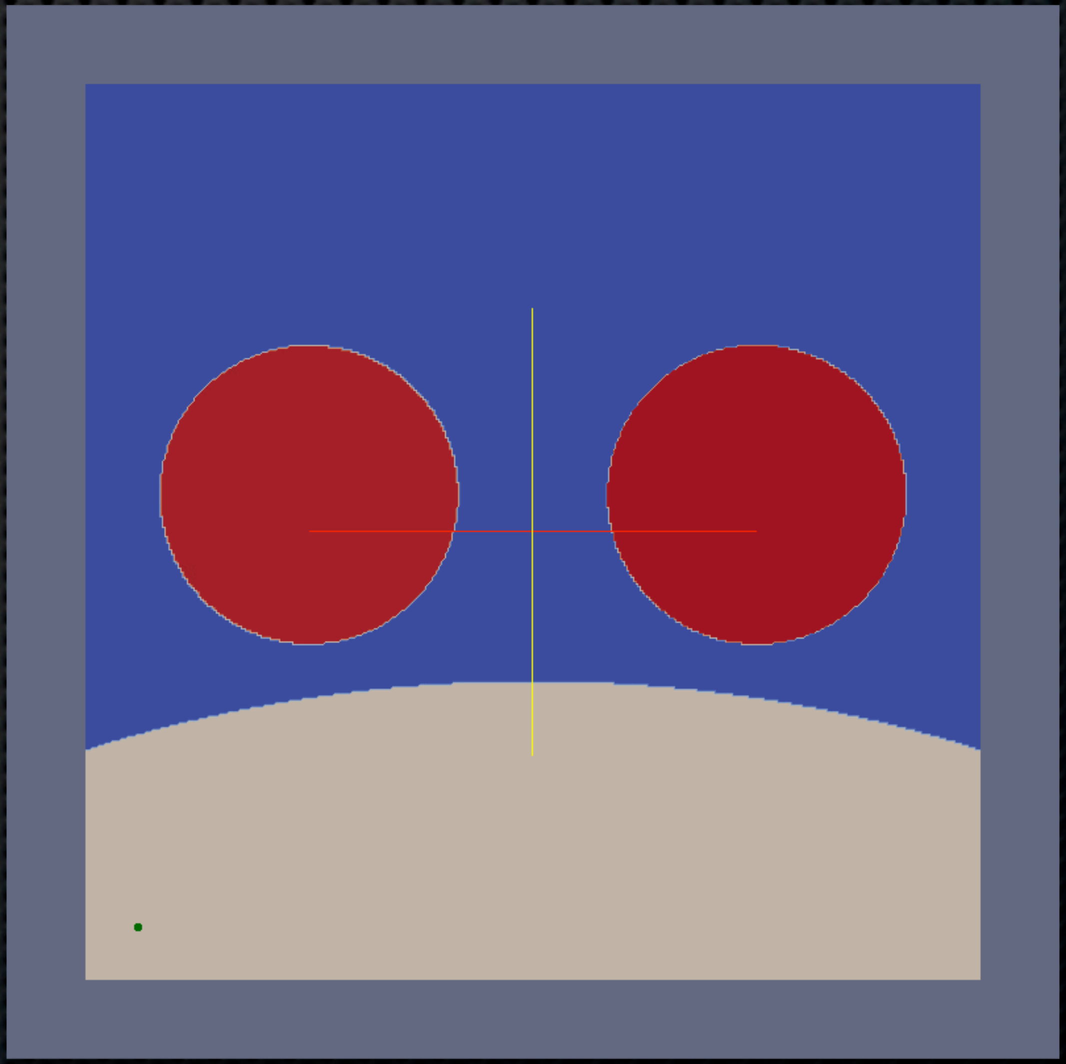

$$\lambda_p = \frac{\mu_p}{\mu_m} \qquad \mathcal{R}^{(p)} = \frac{(\rho_m - \rho_p) g x_c^2}{u_c \mu_m}$$

# Patch Settling

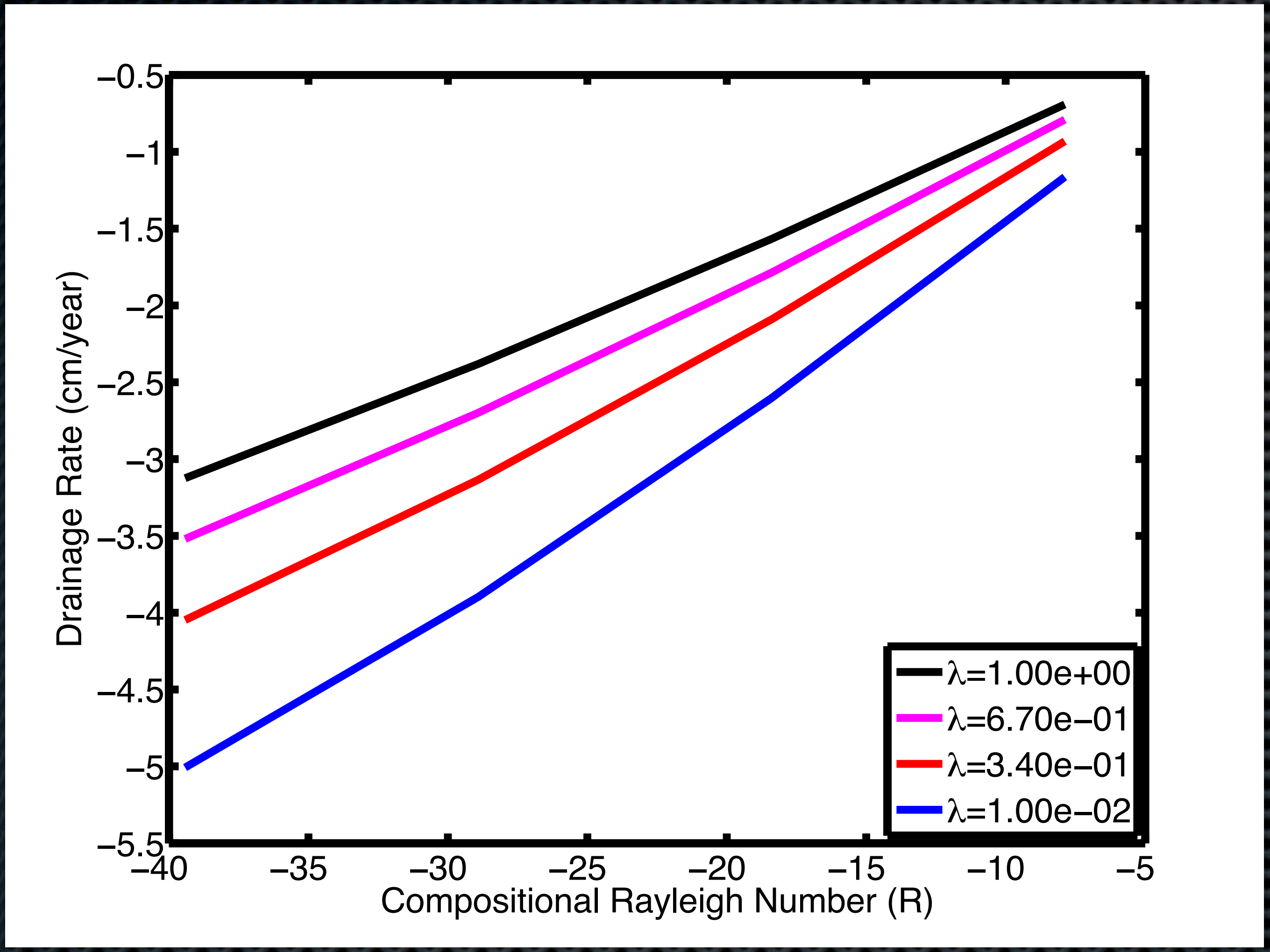


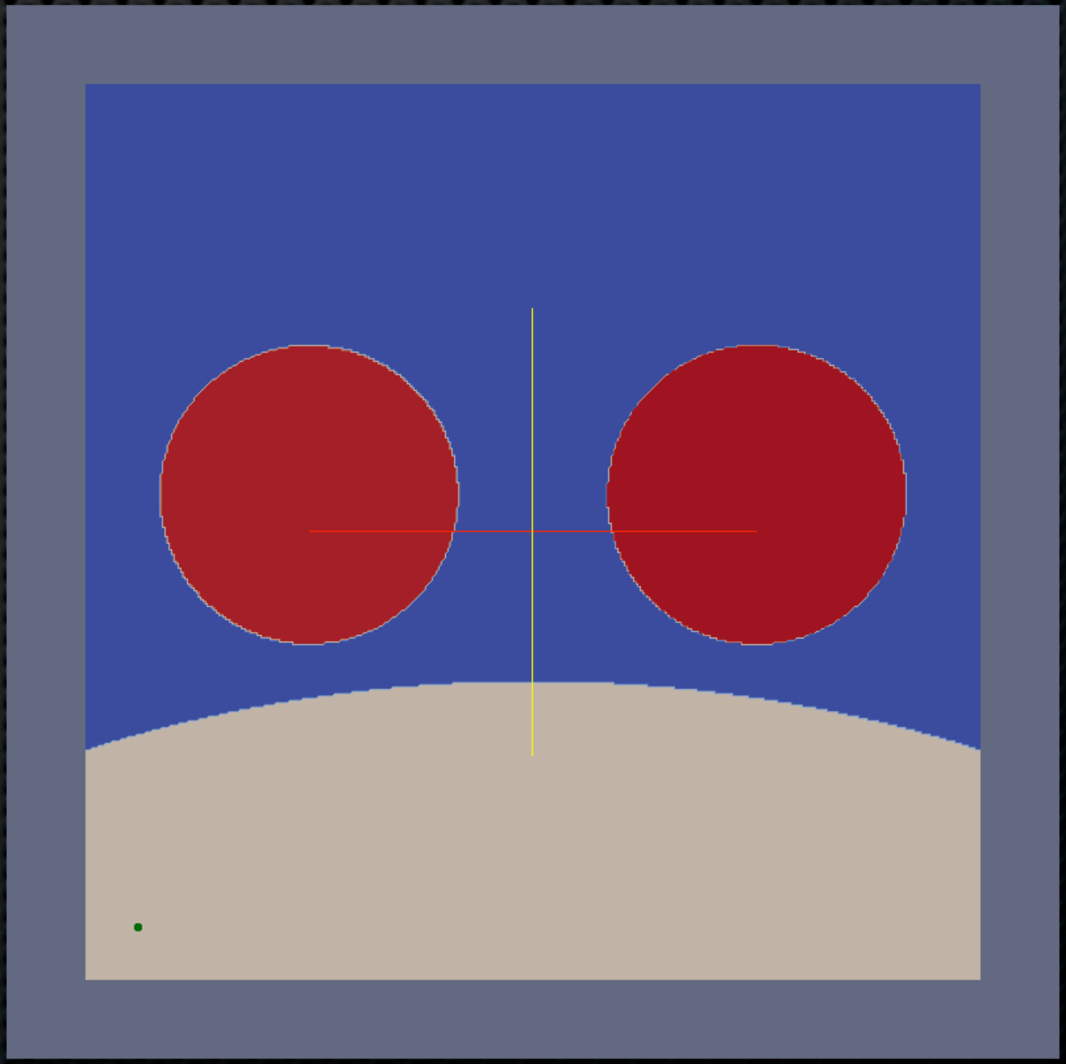

$$\lambda_p = \frac{\mu_p}{\mu_m} \qquad \mathcal{R}^{(p)} = \frac{(\rho_m - \rho_p) g x_c^2}{u_c \mu_m}$$

# Patch Settling

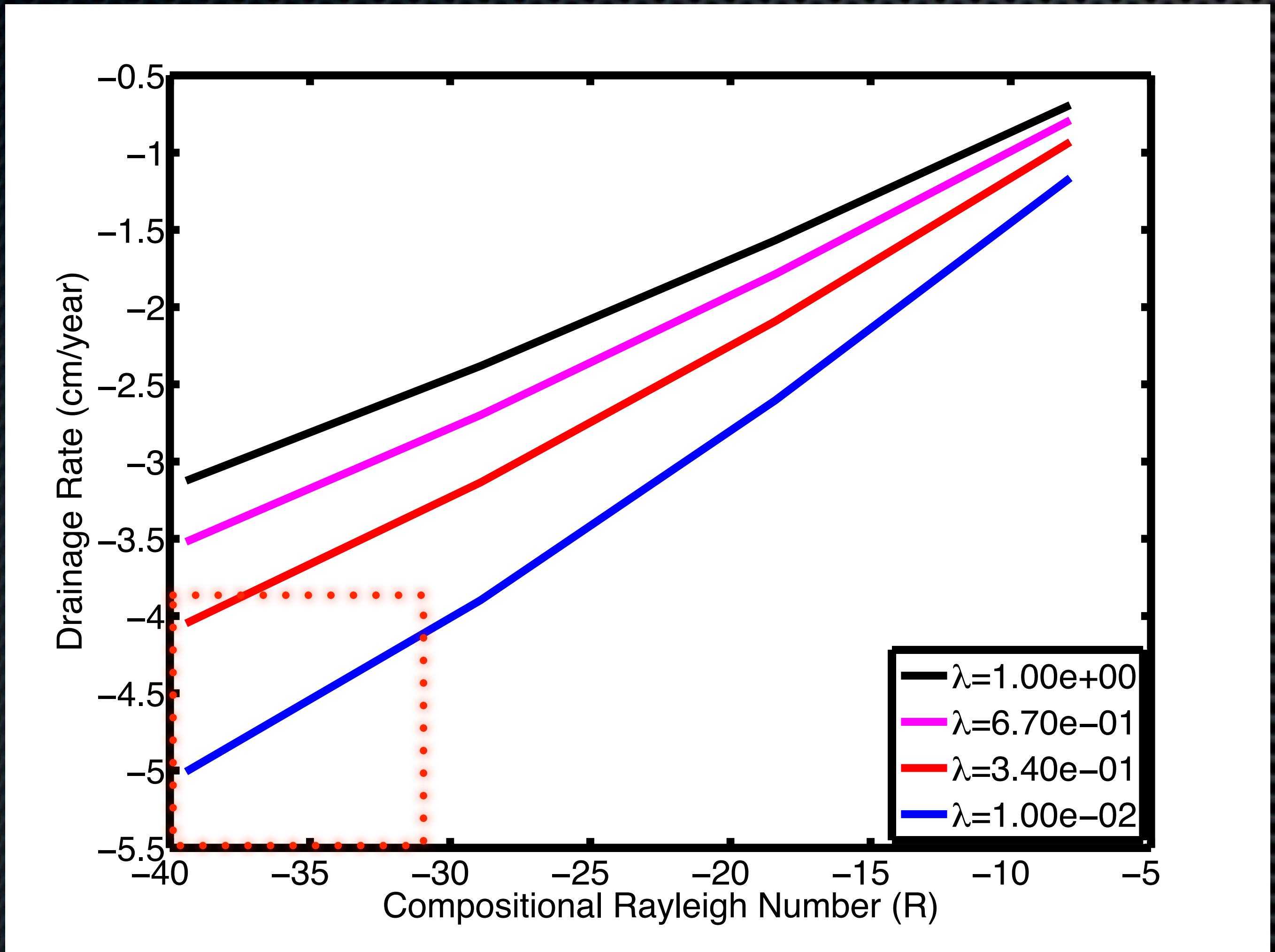


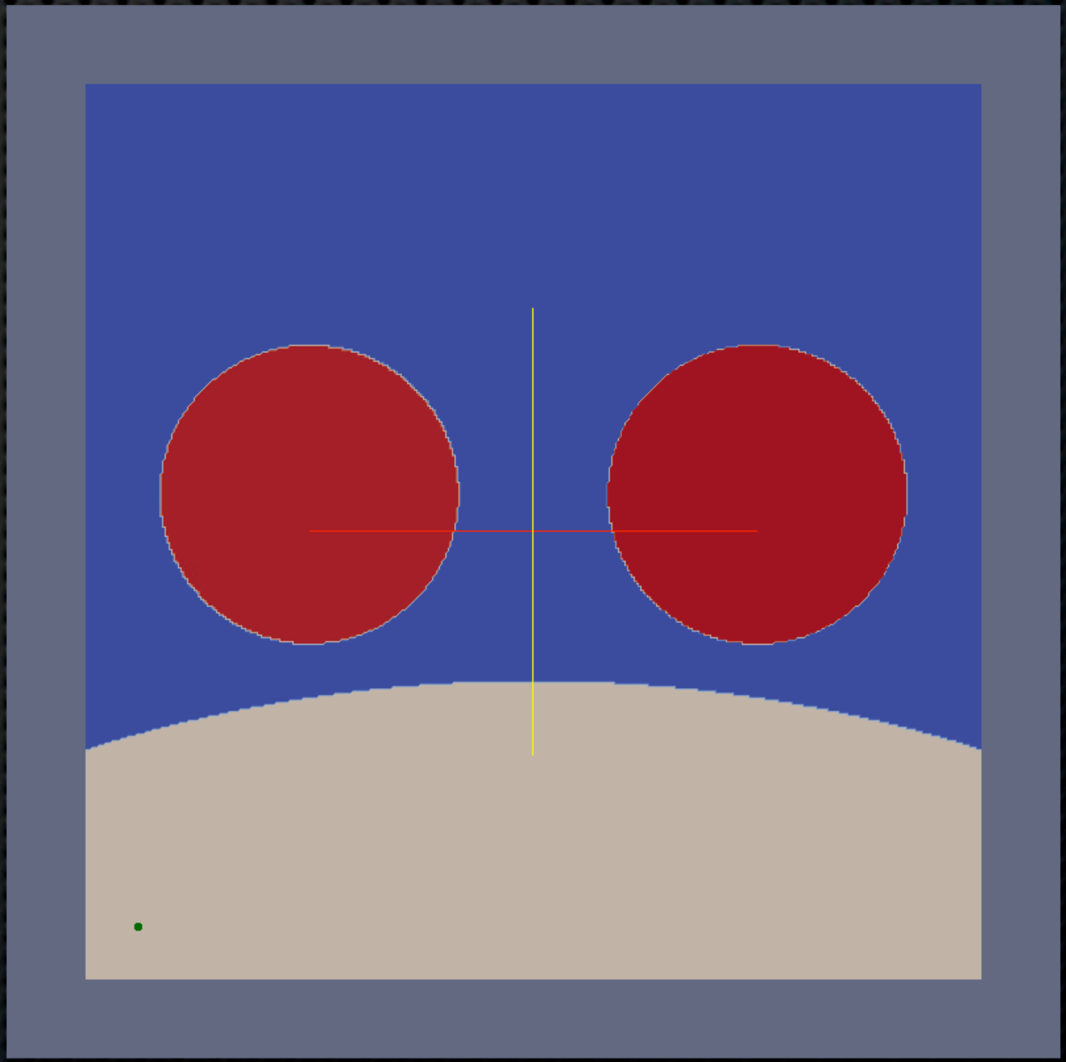

$$\lambda_p = \frac{\mu_p}{\mu_m} \qquad \mathcal{R}^{(p)} = \frac{(\rho_m - \rho_p) g x_c^2}{u_c \mu_m}$$

# ULVZ Simulation #2

Upwell Driven Imposed Flow

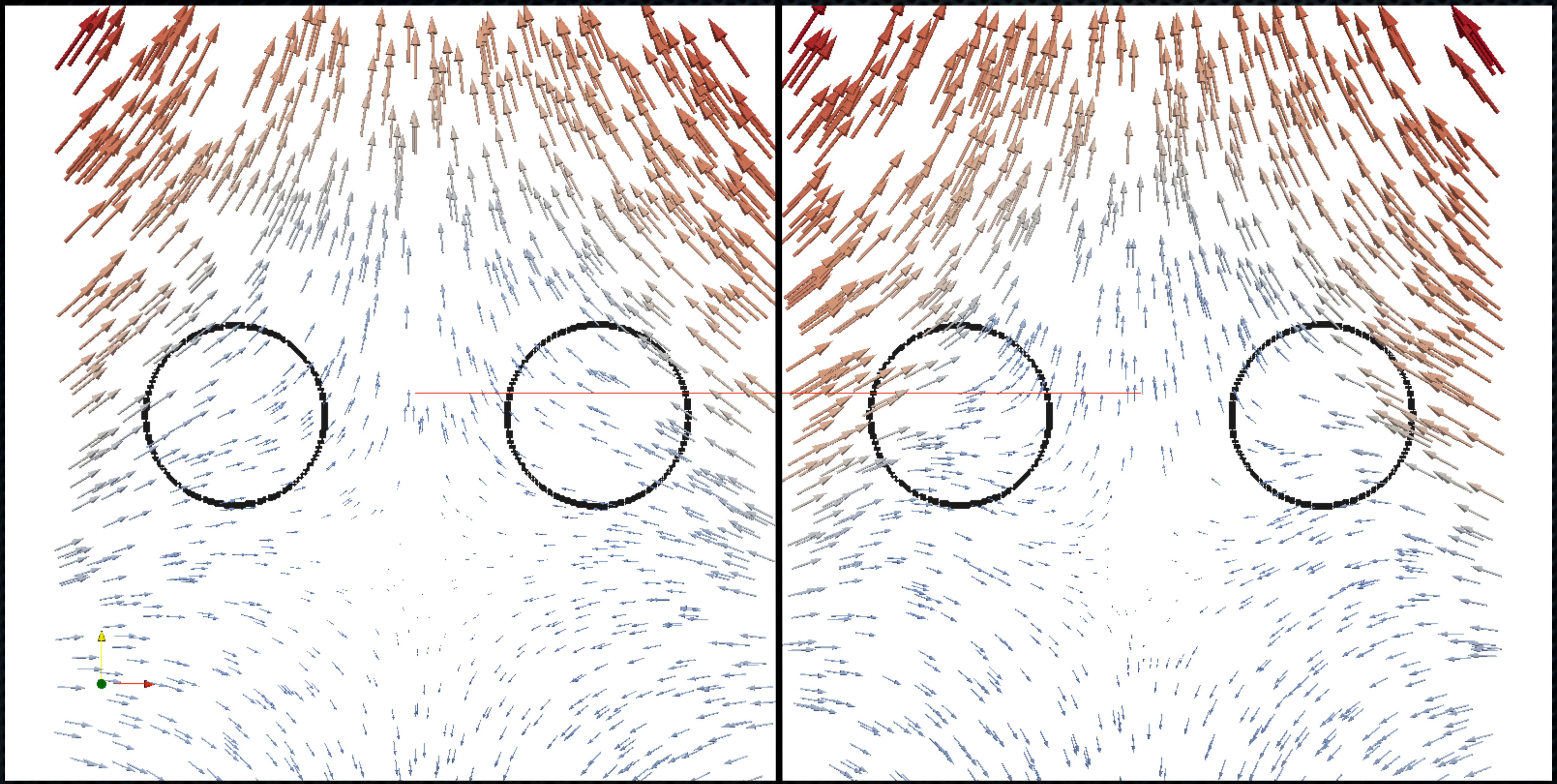

# Upwell Dynamics (10 Myrs)

Left: High patch viscosity

Right: Low patch viscosity

# Summary

- Numerically experimented via FMBEM the ULVZ patch drainage in LLSVP for various densities and viscosities
- Inverse linear relationship between viscosity and drainage rate
- Linear relationship between compositional Rayleigh number and drainage rate
- Interaction of patches leads to asymmetric spreading
- Evidence of core deformation for ULVZ-like parameters

# References


- X. Gao, “Numerical evaluation of two-dimensional singular boundary integrals--Theory and Fortran code”, Journal of Computational and Applied Mathematics, Volume 118, Pages 44-64, 2006
- E.J. Garnero and A.K. McNamara, “Structure and Dynamics of Earth's Lower Mantle”, Science, Volume 320, Issue 5876, Pages 626-628, 2008
- S. Hier-Majumder and J. Revenaugh, “Relationship between the viscosity and topography of the ultralow-velocity zone near the core–mantle boundary”, Earth and Planetary Science Letters, Volume 299, Pages 382-386, 2010
- D.M. Koch and D.L. Koch, “Numerical and theoretical solutions for a drop spreading below a free fluid surface”, Journal of fluid mechanics, Volume 287, Issue 1, Pages 251-278, 1994
- L.G. Leal, Advanced Transport Phenomena: Fluid Mechanics and Convective Transport Processes, Cambridge Series in Chemical Engineering, 2007
- T.M. Lassak et al., “Core-mantle boundary topography as a possible constraint on lower mantle chemistry and dynamics”, Earth and Planetary Science Letters, Volue 289, Pagrs 232-241, 2010
- Y.J. Liu and N. Nishimura, “The fast multipole boundary element method for potential problems: a tutorial”, Engineering Analysis with Boundary Elements, Volume 30, Issue 2, Pages 371-381, 2006

# References


- Y.J. Liu, “A new fast multipole boundary element method for solving 2-D Stokes flow problems based on a dual BIE formulation”, Engineering Analysis with Boundary Elements, Volume 32, Issue 2, Pages 139-151, 2008
- M. Manga and H.A. Stone, “Buoyancy-Driven Interactions Between 2 Deformable Viscous Drops”, Journal of fluid mechanics, Volume 256, Pages 647-683, 1993
- A.K. McNamara, E.J. Garnero, and S. Rost , “Tracking deep mantle reservoirs with ultra-low velocity zones”, Earth and Planetary Science Letters, Volume 299, Pages 1-9, 2010
- C. Pozrikidis, Boundary integral and singularity methods for linearized viscous flow, Cambridge Texts in Applied Mathematics, 1992
- C. Pozrikidis, “Interfacial Dynamics for Stokes Flow”, Journal of Computational Physics, Volume 169, Issue 2, Pages 250-301, 2001
- S. Rost et al., “Seismological constraints on a possible plume root at the core–mantle boundary”, Nature, Volume 435, Issue 7042, Pages 666-669, 2005
- M.S. Warren and J.K. Salmon, “A Parallel Hashed Oct-Tree N-Body Algorithm”, Proceedings of the 1993 ACM/IEEE conference on Supercomputing, AMC, Pages 12-21, 1993

DI22A-08

# Dynamics of ULVZ-mantle interaction using fast multipole boundary element method

NSF EAR 0911094 and EAR 1215800

Tyler Drombosky - `drombosk@math.umd.edu`

University of Maryland College Park

Applied Mathematics and Scientific Computation

Saswata Hier-Majumder - `saswata@umd.edu`

University of Maryland College Park

Department of Geology

Center for Computational Sciences and Mathematical Modeling

# Extra Slides

## FMM Expansions

# Validity of Expansion

- Expansions are valid based on the $L_2$ distance between boundary elements and Greens functions
- Distance matrices cost $\mathcal{O}(N^2)$ time and space to compute
- Approximate distances using $L_1$ norm to determine areas of validity
- A Morton number scheme is used to greatly accelerate the process [Warren 1993]

x=0.01010101110
y=0.10111010100
01100111011001

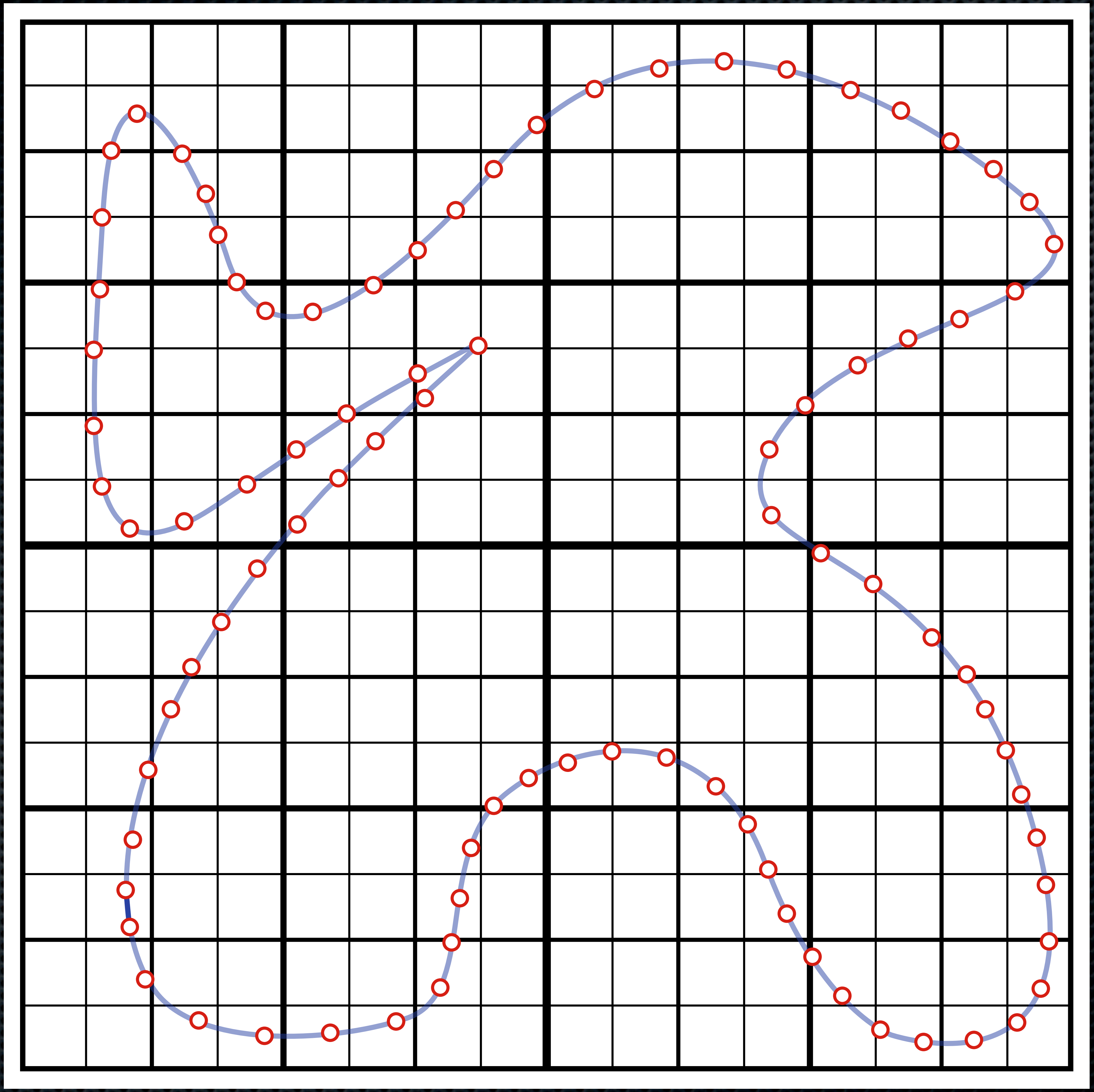

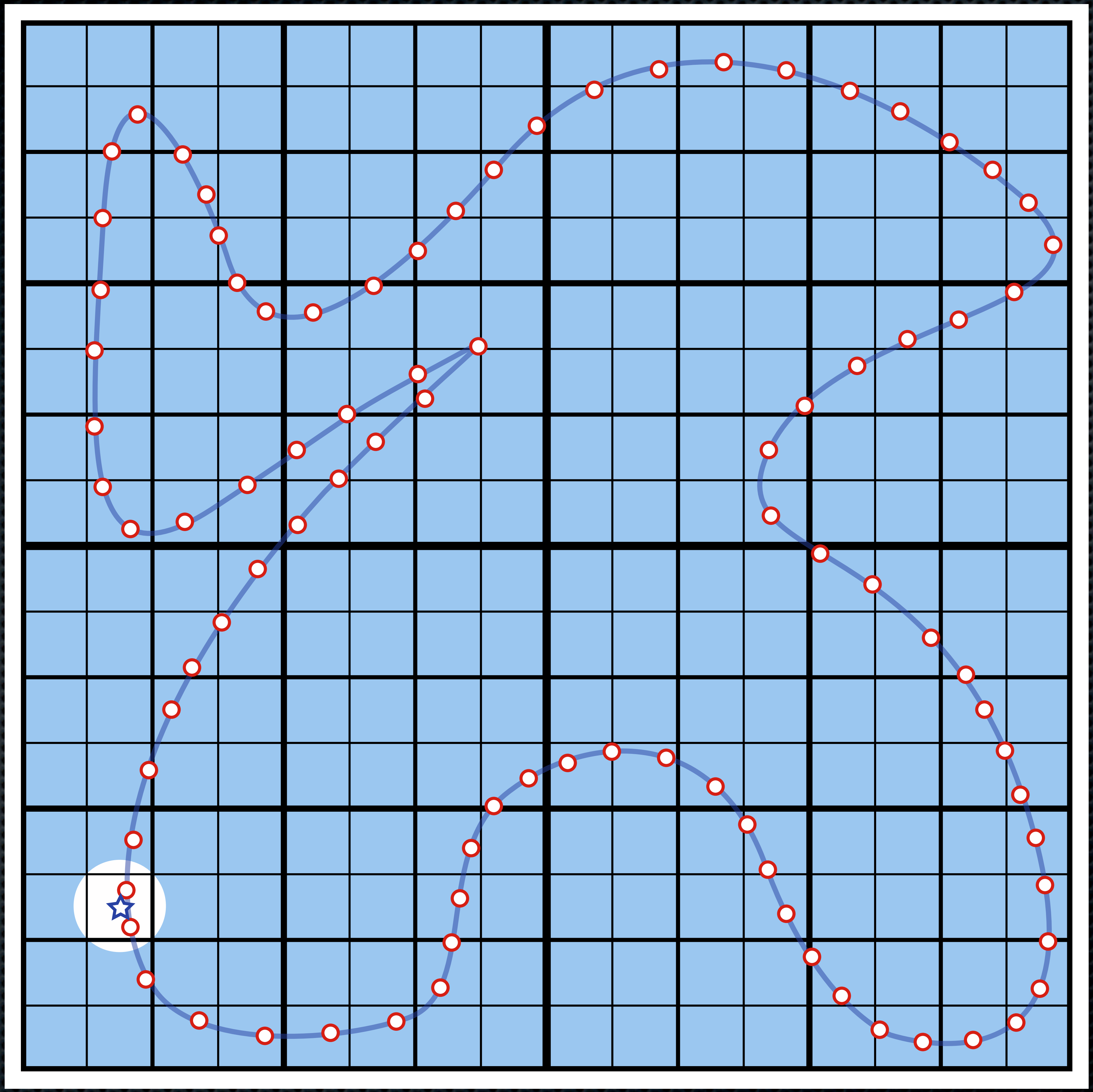

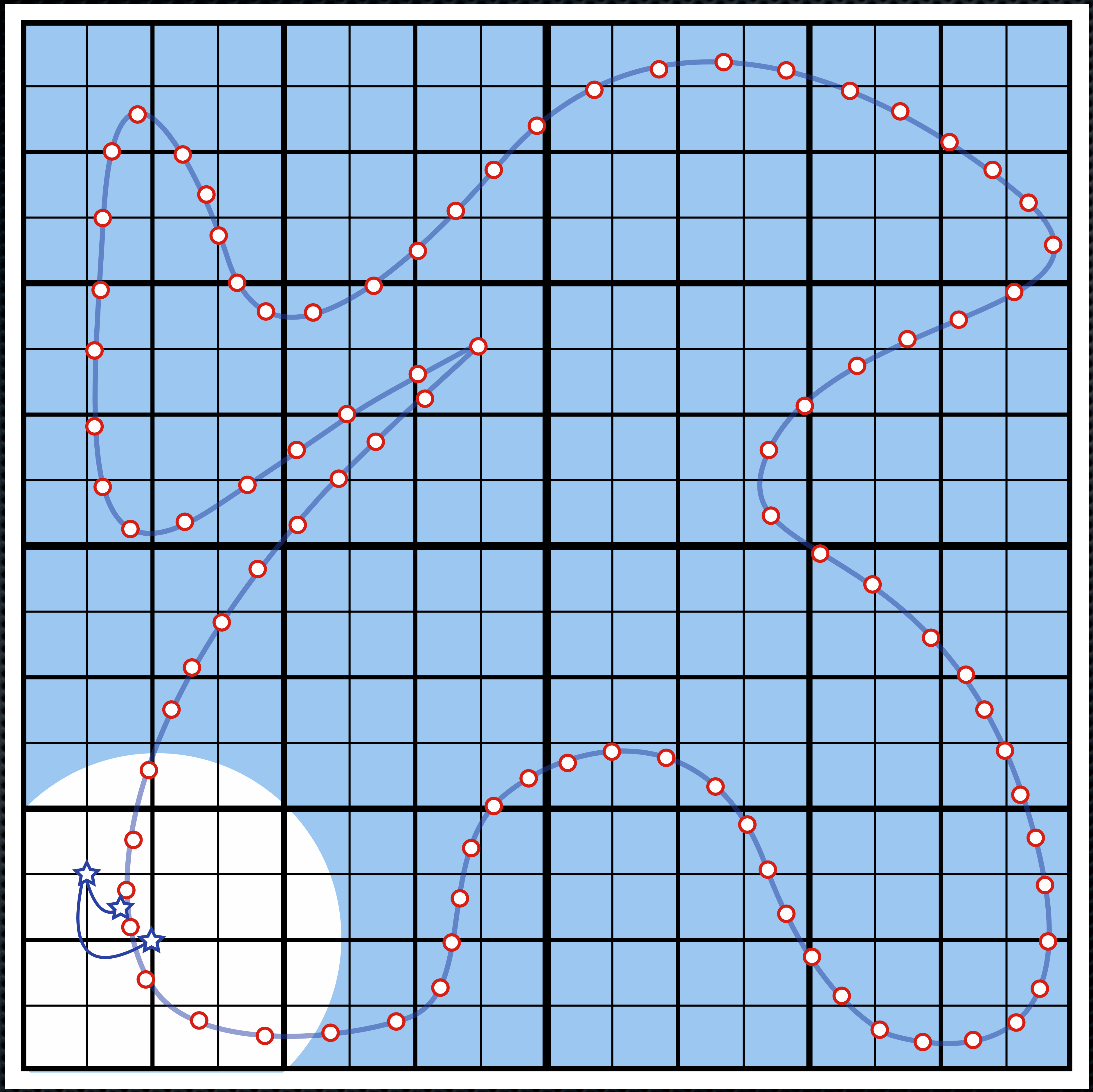

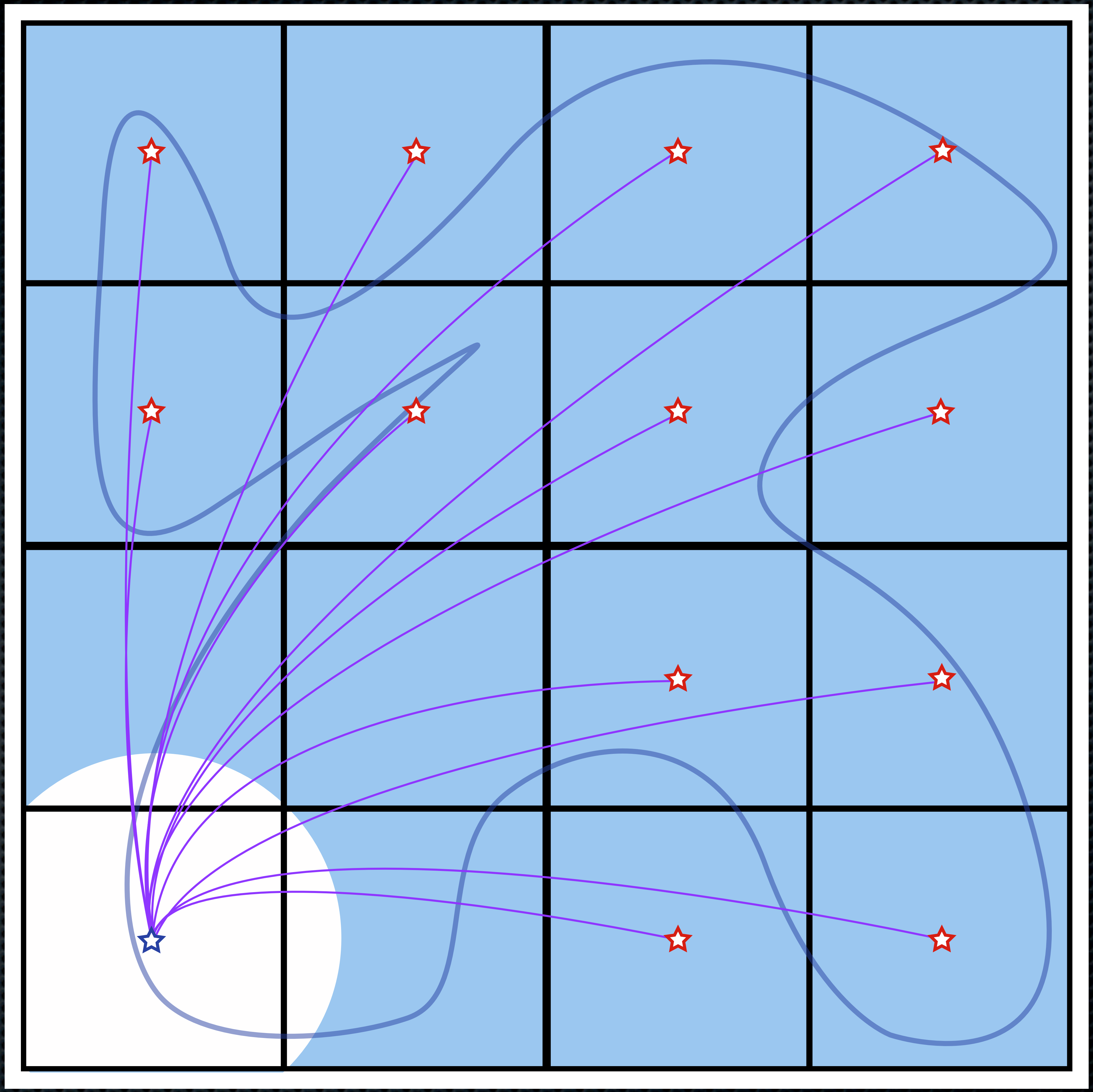

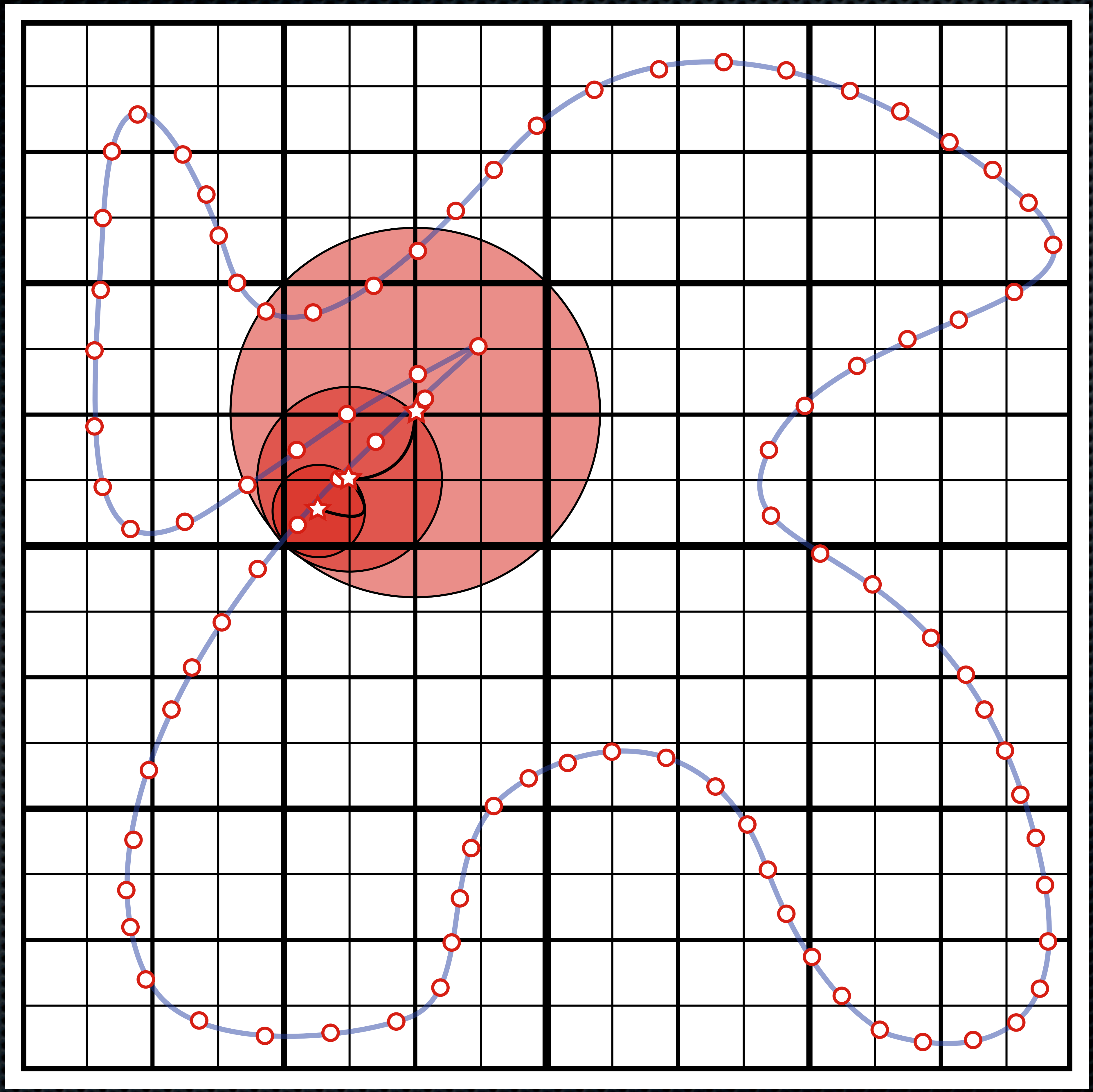

# Extra Slides

CMB 4x4 Simulation

# Settling Interaction

- Two ULVZ patches are placed above a core
  - The viscosity ratio and density contrast of the patches with respect to the mantle is varied
  - The viscosity ratio parameter ranges from 1e-2 to 1
  - The density of the patches are varied 2-8% more dense than the mantle
  - Simulations are run for 5 million years

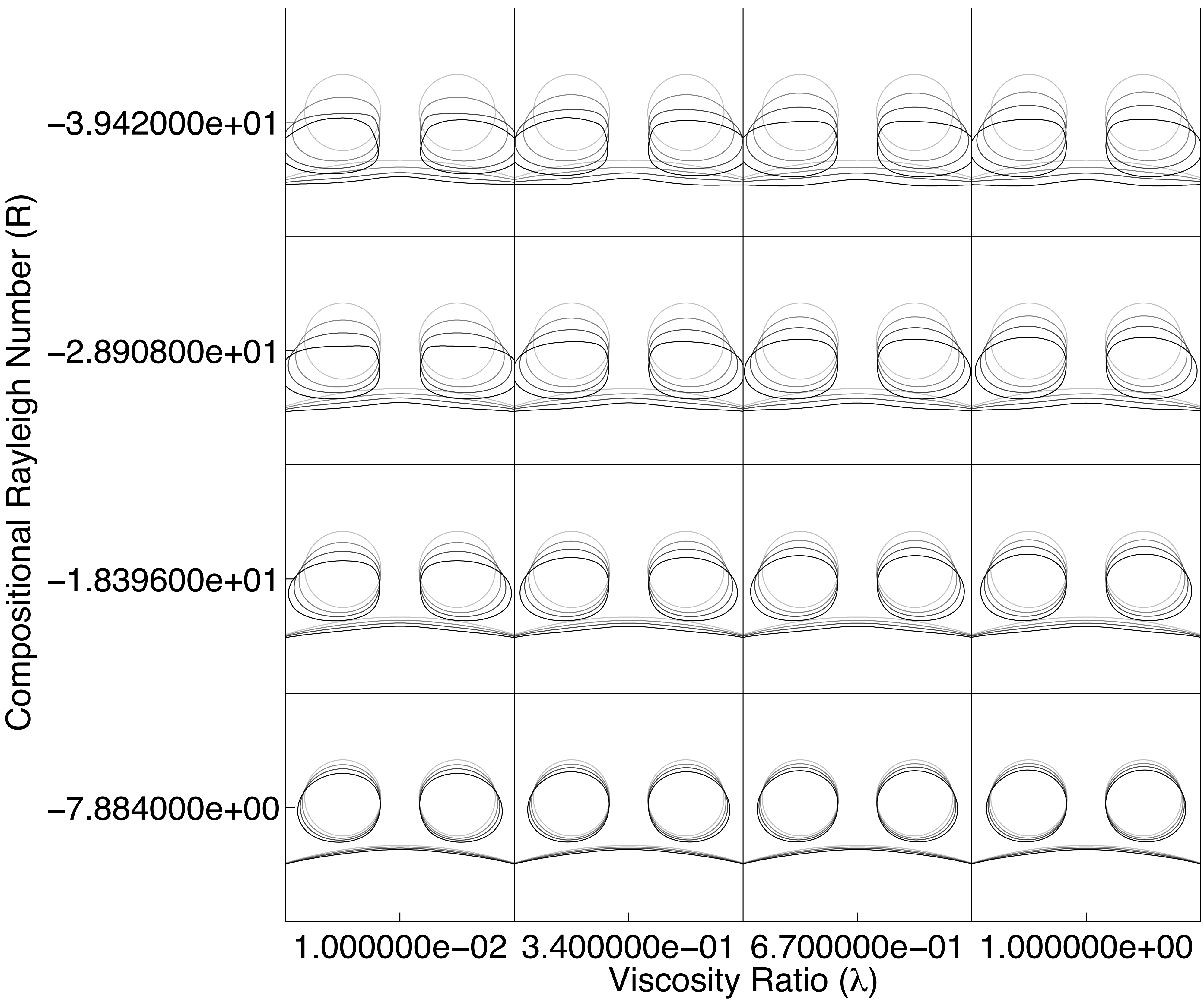

Compositional Rayleigh Number (R)
−3.942000e+01
−2.890800e+01
−1.839600e+01
−7.884000e+00
1.000000e−02
3.400000e−01
6.700000e−01
1.000000e+00
Viscosity Ratio (λ)

# Extra Slides

Imposed Flow Simulation

# Rising Interaction

- Two patches are placed in an upswell imposed velocity similar to a plume.
  - The viscosity ratio and density contrast of the patches with respect to the mantle is varied
  - The viscosity ratio parameter ranges from 1e-2 to 1
  - The density of the patches is varied between 102% and 110% of mantle density
  - Simulations are run for 5 million years

# Rising Analysis

- For low compositional Rayleigh number, solution is dominated by the imposed velocity field
- For moderately size compositional Rayleigh numbers the upswell is able to support some or all of the patch
- With large compositional Rayleigh numbers the density contrast of the patch overcomes the imposed velocity
- For all compositional Rayleigh numbers low viscosity ratios allows the patch to deform easily in the direction of greatest velocity

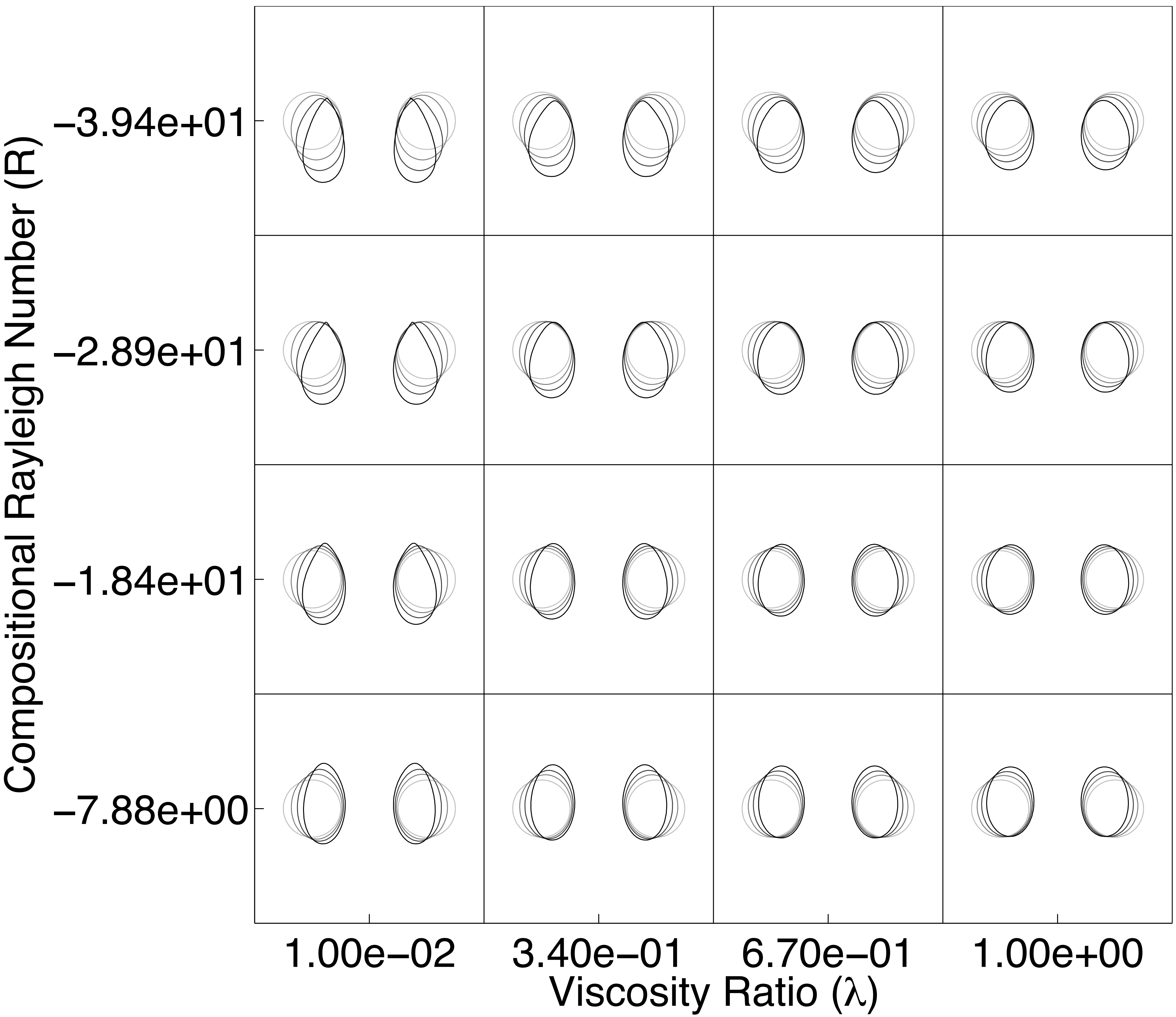

Compositional Rayleigh Number (R)
−3.94e+01
−2.89e+01
−1.84e+01
−7.88e+00
1.00e−02
3.40e−01
6.70e−01
1.00e+00
Viscosity Ratio (λ)

# Patch Interaction

- Velocity is able to uplift part of the particles
- In low velocity regions, gravitational force overcomes
- As particles approach, pressure builds and velocities repel
- No spreading due to lack of lower boundary

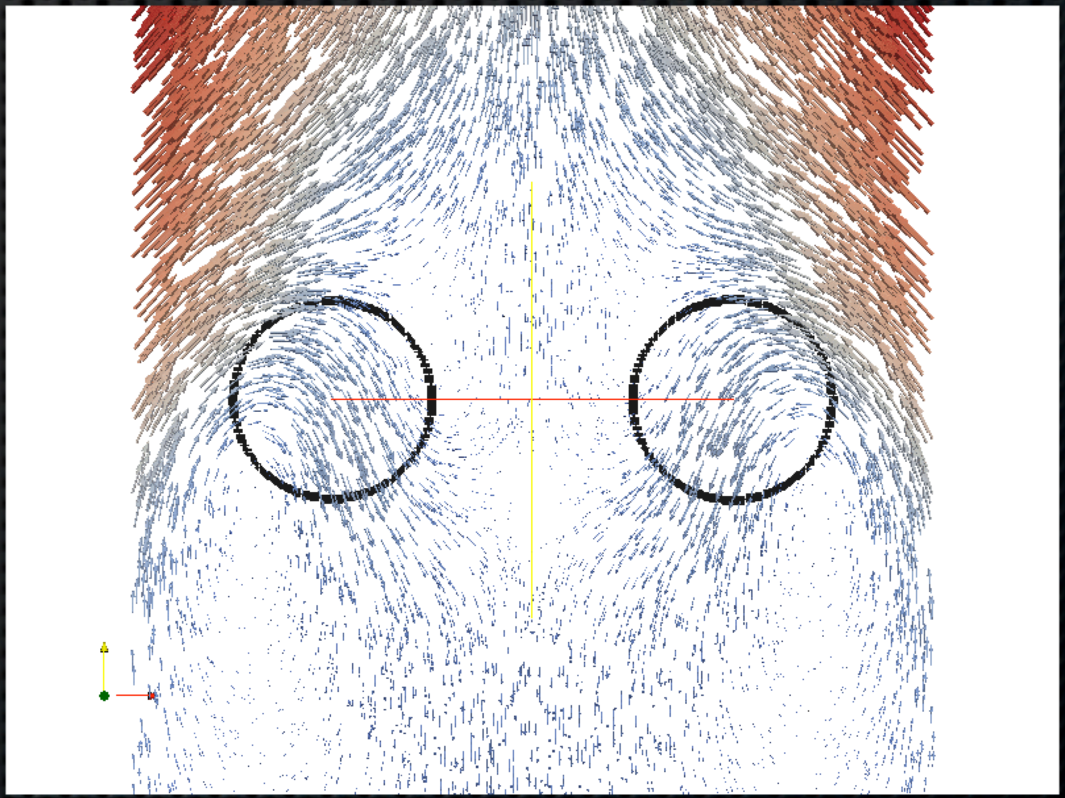

# Extra Slides

## Evidence Of Core Deformation

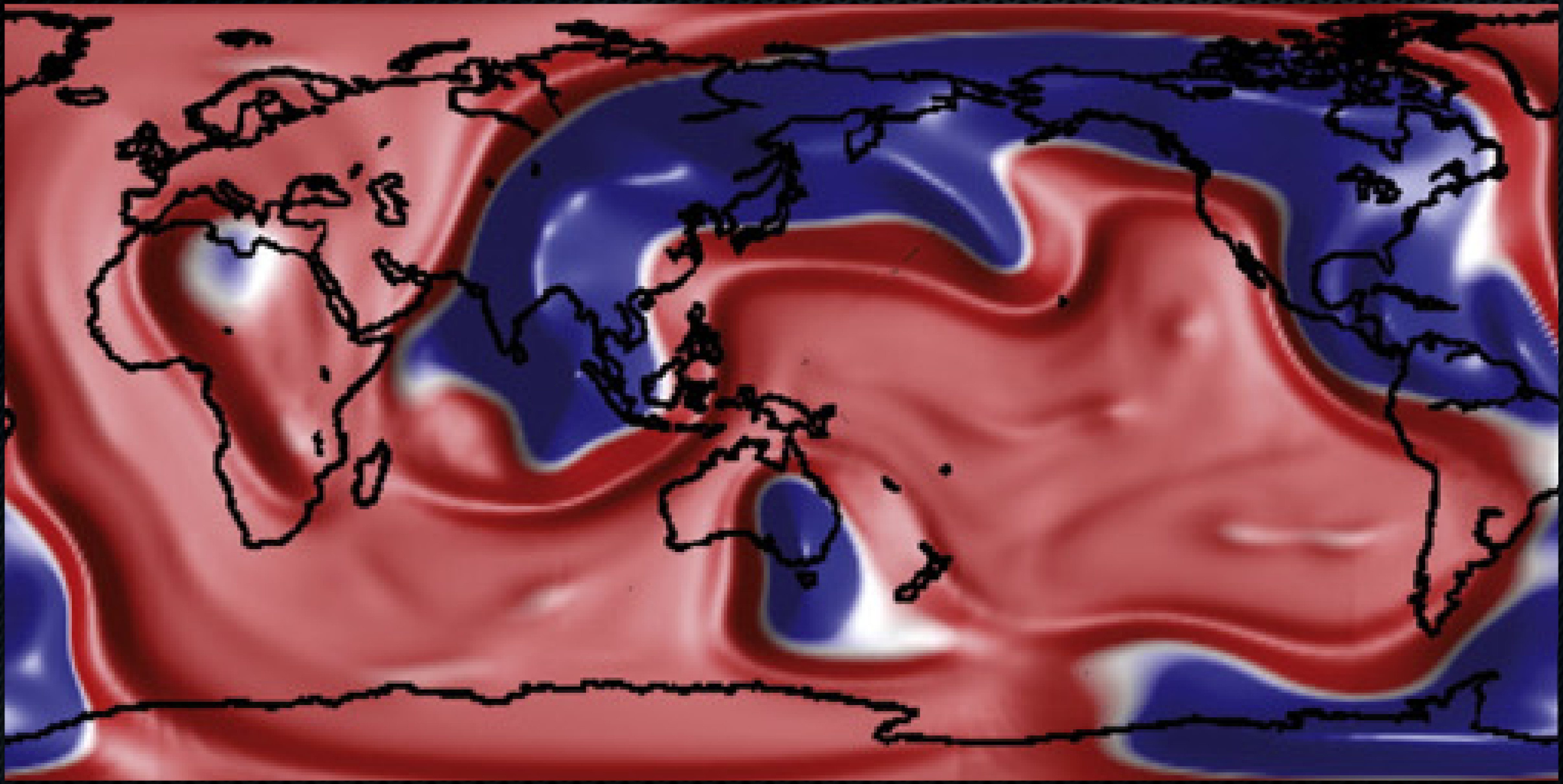

[Lassak et al. 2010]

Numerical model of core mantle boundary shows deformation in areas of detected ULVZs.